Multifunctional Electrospun Biocompatible Nanofiber Composites from Water Dispersion Blends of Folic Acid Conjugated PVP/Dextran/ODA-MMT Nanocomposites and Their Responses to Vero cells

Folik Asit Konjuge Edilmiş PVP/Dekstran/ODA-MMT Nanokompozitlerin Sulu Dispersiyon Karışımlarından Üretilen Çok Fonksiyonlu Elektroeğrilmiş Biyouyumlu Nanofiber Kompozitler ve Bunların Vero Hücreleriyle Etkileşimi

Research Article

Murat Şimşek[1], Zakir M. O. Rzayev[2*], Ulviya Bunyatova[3], Sevda Khalilova[4], Mustafa Türk[5]

[1]Department of Biomedical Engineering, Faculty of Engineering, İnönü University, Malatya, Turkey.
[2]Department of Nanotechnology and Nanomedicine, The Institute of Science, Hacettepe University, Turkey.
[3]Department of Biomedical Engineering, Faculty of Engineering, Başkent University, Ankara, Turkey.
[4]Scientific Research Institute of Medicinal Prophylaxis, Ministry of Public Health, Baku-Sumgait, Azerbaijan.
[5]Department of Bioengineering, Faculty of Engineering, Kırıkkale University, Kırıkkale, Turkey.

ABSTRACT

This work presents the fabrication and characterization of novel colloidal multifunctional polymer nanofiber composites (NFCs) from water dispersion blends of the intercalated silicate layered nanocomposites of poly(2-vinyl-N-pyrrolidone)/octadecyl amine-montmorillonite (PVP/ODA-MMT) and Dextran/ODA-MMT as matrix and partner polymer intercalated nanocomposites, as well as their folic acid (FA) conjugated derivatives by reactive electrospinning. The chemical and physical structures, surface morphology and responses to Vero cells of NFCs were investigated. Effects of matrix/partner polymer volume ratios, composition, organoclay and FA on the main important parameters of NFCs were evaluated. Cell culture studies showed that NFCs did not exhibit cytotoxicity significantly and also had a low degree of apoptotic and necrotic effects.

Key Words
PVP, dextran, nanofiber, folic acid, organoclay, nanocomposite.

ÖZ

Bu çalışma matris ve partner polimer nanokompozitler olarak poli(2-vinil-N-prolidon)/okdadesil amin-montmorillonit (PVP/ODA-MMT) ve Dekstran/ODA-MMT sulu dispersiyon karışımlarından ve aynı zamanda bunların folik asit (FA) konjuge edilmiş türevlerinden kolloidal çok fonksiyonlu polimer nanofiber kompozitlerin (NFC) reaktif elektroeğirme yöntemi ile fabrikasyonunu ve karakterizasyonunu sunmaktadır. NFC'lerin kimyasal ve fiziksel yapıları, morfolojileri ve Vero hücrelerine olan cevapları araştırılmıştır. Matriks/partner polimer oranının, bileşiminin, organokilin ve FA'nın NFC'lerin ana parametreleri üzerindeki etkileri değerlendirilmiştir. Hücre kültür çalışmaları NFC'lerin önemli bir toksik bir etki sergilemediklerini ve ayrıca düşük seviyede apoptotik ve nekrotik etkiye sahip olduklarını göstermiştir.

Anahtar Kelimeler
PVP, dekstran, nanofiber, folik asit, organokil, nanokompozit.

Article History: Received: Apr 30, 2016; Revised: Jun 15, 2016; Accepted: Jun 20, 2016; Available Online: Dec 31, 2016.

DOI: 10.15671/HJBC.2016.125

Correspondence to: Z. M. O. Rzayev, Department of Nanotechnology and Nanomedicine, The Institute of Science, Hacettepe University, Turkey.
Tel: +90 312 297 7400 Fax: +90 312 299 2124 E-Mail: razayevzmo@gmail.com

INTRODUCTION

Over the last years, attention of many researchers has focused on fabrication of synthetic and natural polymer nanofibers from solution blends of various polymers and/or polymer nanocomposites as a binary multifunctional matrix/partner polymer systems rather than fabricating nanofiber structures from one polymer. Polymer nanofibers fabricated by electrospinning method are preferred because of their unique properties, such as high surface area-to-volume ratio, high functionality, nanoscale fiber diameter and nanoporous surface morphology [1-5]. The phase separation process during electrospinning and properties of fabricated nanofibers strongly depend on the applied parameters, matrix partner polymers compatibility, chemical and physical structural factors and various interactions such as hydrogen bonding, complex formation and different chemical reactions between the functional groups of both polymers.

Poly(2-vinyl-N-pyrrolidone) (PVP) having very important properties such as biocompatibility, low toxicity, complexion stability, relatively inert and adhesive behaviors, and resistant to thermal degradation has several applications in pharmaceutical, food, beverage, cosmetic, and photographic industries [6]. It has been also extensively used as a template for preparing functional nanofibers for several applications [7,8].

Dextran is a polysaccharide-based biopolymer with excellent biocompatibility and biodegradability properties. It has several applications in biomedical such as carriers for drug delivery [9,10] scaffolds for cell and tissue engineering [11,12], and biosensors [13,14]. It is also a versatile biomacromolecule for preparing electrospun nanofiber membranes by blending with either water-soluble bioactive agents or hydrophobic biodegradable polymers for biomedical applications [15,16]. Jiang et al. [17] optimized and characterized dextran-based nanofiber membranes prepared by electrospinning.

Folic acid (FA) is a water-soluble B vitamin, and as a multifunctional organic compound contains reactive primary and secondary amine and two carboxylic groups, as well as ionizable methylpteridin and aminobenzoic rings. Various FA derivatives have biological activities [18]. FA is also used for preventing to DNA and, thus for preventing cancer cells, and served as antibiotics and cytotoxic drugs in the treatment of cancer, bacterial and protozoal infections [19]. Bongartz et al. [20] reported the preparation, characterization and application of folic acid modified montmorillonite clay as a cell culture material. FA was used as a modifier to facilitate adhesion of folate positive cells on the clay surface. A FA modified poly(ε-caprolactone)/MMT intercalated nanocomposite was prepared and characterized as a cell culture and biosensing platform [21]. Jiang et al. [22] synthesized of carboxymethyl dextran terminated Fe_3O_4 magnetic nanoparticles and their conjugations with FA as the promising materials for local hyperthermia treatment therapy and the magnetic resonance imaging *in vitro* and *in vivo*.

Unlike polysaccharide based layered silicate bionanomaterials, the dextran/organoclay nanocomposites and nanofibers and their folic acid conjugated complexes were scarcely investigated. Fabrication and characterization of carboxylate methylcellulose (CMC), starch-g-PLA, poly (maleic anhydride-*alt*-1-octadecene)-g-PLA, poly(vinyl alcohol), poly(ε-caprolactone) and CMC based silicate layered nanocomposites and nanofibers were subjects of our recent publications [23-26]. In this work, the synthetic pathways for fabrication of PVP and dextran based silicate layered multifunctional nanofibrous structures and their FA conjugated complexes were described. Effects of composition (fraction of dextran partner biopolymer), loading and FA on the chemical and physical structures of biocompatible NFCs were evaluated. A special attention would focus on *in situ* chemical and physical interfacial interactions during reactive electrospinning processing, and their responses to Verol cell lines.

EXPERIMENTAL

Materials

PVP with average M_w = 360.000 Da), Dextran with average M_w = 64.000-76.000 Da and reactive ODA-MMT (Nanomer I.30E, Nanocor Co.) with the following average parameters: content of ODA surfactant-intercalant 25-30%, particle size 8-10 µm, bulk density 0.41 g/cm^3, crystallinity 52.8 % (by XRD) and *d*-spacing 19.22 Å at 4.05° 2θ angle; and FA (≥ 97) with molecular weight of 441.4 Da were purchased from Sigma-Aldrich (Germany).

Vero (kidney epithelial cells of rodent) cell line was obtained from the Tissue and Cell Culture Bank of the Foot and Mouth Disease Research Institute (Ankara, Turkey). Cell culture flasks and other plastic materials were purchased from Corning (USA). The growth medium, Dulbecco Modified Medium (DMEM) without L-glutamine supplemented with fetal calf serum, and Trypsin-EDTA were purchased from Biological Industries (USA). 2-(4-iodophenyl)-3-(4-nitrophenyl)-5-(2,4-disulfo-phenyl)-2H-tetrazolium, monosodium salt (WST-1) was purchased from Roche (Germany). Hoechst 33342 and propodium iodide (PI) were purchased from Serva (Israel). Phosphate buffer solution (PBS) was purchased from Sigma-Aldrich (USA). Other chemicals used were analytically grade.

Synthesis of NFCs by Green Electrospinning

Synthesis of matrix PVP/ODA-MMT (NC-1) and partner dextran/ODA-MMT (NC-2) nanocomposites were carried out by intercalating PVP and dextran macromolecules between ODA-MMT (content of loaded clay for PVP and dextran is 3.5%) layered silicate galleries by dispersing with intensive mixing in distilled water medium at room conditions up to formation homogenous viscose products. Pure water solutions of NC-1/NFC-2 nanocomposites with different volume ratios and their FA (1.0 mass %) incorporated derivatives were used to fabricate nanofiber mats by the electrospinning method. In brief, 6 mL NC-1 (22 mass %) and 4 mL NC-2 (50 mass %) were mixed until homogeneous product was obtained at room temperature. Then, the polymer solution was loaded into a 2.5 mL plastic syringe equipped with a stainless steel needle. The nanofibers from NC-1 and NC-1/NC-2 solution blends with different volume ratios (8/2, 6/4 and 8/2-FA v/v) were fabricated in the optimized electrospinning conditions: a flow rate of 0.5 mL/h; a high voltage of 18 kV; a distance of 17 cm between the tip of the needle and the grounded collector. Randomly oriented fibers were obtained by collecting fibers onto an aluminum foil fixed on a stationary collector.

Characterizations

Fourier Transform Infrared (FT-IR) spectra were recorded on a Thermo-Nicolet 6700 spectrometer in the range of 4000-500 cm^{-1} with a resolution of 4 cm^{-1}.

The X-ray powder diffraction (XRD) patterns were performed with a PANANALYTICAL X-ray diffractometer equipped with a CuK tube and Ni filter (λ = 1.5406 Å). The XRD patterns and reflection parameters were measured using a range of 1-70° 2θ angle. The Bragg equation was used to calculate the interlayer spacing (d): $n\lambda = 2d\sin\theta$, where n is the order of reflection, and θ is the angle of reflection.

The surface morphology of nanofiber films was examined using a Scanning Electron Microscope (SEM, ZEISS SUPRA 40). All specimens were freeze dried and coated with a thin layer of platinum before testing by using a QUORUM-Q150R ES coating device.

In Vitro Cell Culture Expriments

Cytotoxicity

The WST-1 assay was used to evaluate cell cytotoxicity, proliferation and viability. Nanofiber samples were sterilized with UV for 30 min prior to use. Vero cells were seeded into 96-well microassay plates at a concentration of 5 × 10^3 cells/well and incubated 24 hours at 37°C. Samples from volume ratios of 8/2 of NC-1/NC-2 (NFC-8/2), 6/4 of NC-1/NC-2 (NFC-6/4) and 8/2-FA of NC-1/NC-2-FA (NFC-8/2-FA) (12,5, 25, 50, 100,200 and 400 µg/ml) were added into the cell culture medium and additional inoculation was performed for 48 h at 37°C. The cell culture medium in each well was then replaced with 100 µl of fresh medium and 15 µl of WST-1 solution. After incubating for another 4 h at 37°C in a

dark condition, the wells were read at 440 nm using an ELISA plate reader (Biotek), and then the percentage of viable cells was calculated. For WST-1 assay, the viability of control vero cells was defined as 100 . The medium without fiber samples was indicated as a control. The control samples were reevaluated for each group.

Analysis of Apoptotic and Necrotic Cells

Double staining with Hoechst dye and PI was conducted to quantify the number of apoptotic cells. Vero cells (25×10^3 cells/well) were seeded into 24-well plates containing DMEM cell culture medium. The cells were treated with different concentrations (given above) of nanofiber mats for 48 hours, and then attached and detached cells were harvested. Upon PBS wash, the cells were incubated with Hoechst dye (2 mg/mL), PI (1 mg/mL) and DNAse free-RNAse (100 mg/mL) for 15 min at room temperature. Then, 10-50 mL of cell suspension was smeared on a glass slide and coverslips for imaging under a fluorescence microscope with DAPI and FITC filters (Leica, DMI 6000). In double staining method with Hoechst dye and PI, the nuclei of normal cells are stained with dark blue, while apoptotic cells are stained light blue. The apoptotic cells were identified by their nuclear morphology based on nuclear fragmentation or chromatin condensation. Necrotic cells were stained red by PI. For necrotic cells which are lack of plasma membrane integrity, PI dye can cross the cell membrane. However, it cannot cross an intact cell membrane. The number of apoptotic and necrotic cells in 10 random microscopic fields (about 1000 cell) were counted. Data were showed as the ratio of apoptotic or necrotic cells to normal cells. Each group was triplicated.

RESULTS AND DISCUSSION

Synthetic Pathways of NFCs and Mechanism of Complex-formation and Grafting Reactions

The excellent complexing properties of all used materials in NFCs allowed us to propose the following physical (predominantly) and chemical reactions which occurred before and during electrospinning: (1) PVP and dextran polymer-polymer interaction via acceptor (pyrrolidone unit)-donor (-OH and –O- ether links); (2) complexing the organoclay with dextran and FA through —NH_2...O-ether and —NH_2...HOOC— hydrogen bonding, respectively; and (3) complexing the PVP and dextran macromolecules with FA via —OH...HOOC— strong hydrogen bonding. It was also proposed that the chemical esterification reactions between dextran polymer chains (—OH) and FA (—COOH), as well as amidization of FA with organoclay consisting reactive secondary amine group could be occur during electrospinning process. Some complexing reactions are schematically represented in Figure 1.

Chemical and Physical Structures

The chemical structures of NFCs were confirmed by FT-IR spectroscopy (Figure 2). Agreeing to these results, FT-IR spectral information can be divided the following main absorption band regions: (1) 3700-3000 cm^{-1} region contained the high broadening peaks from N-H and OH stretching bands at 3408 cm^{-1} (Figure 2A) and at 3331 cm^{-1} (Figure 2E) in PVP/ODA-MMT and dextran/ODA-MMT nanofibers, respectively. These bands were shifted to low (N-H for 22 cm^{-1}) and high (-OH for 55 cm^{-1}) regions in NFCs (Figure 2B, C and D). This observed phenomenon can be estimated as physical (hydrogen bonding and complexing) and partially chemical (amidization and esterification) interactions of reactive organoclay and FA with matrix/partner polymer chains via NH_2...HOOC— O=C—NH...OH— and O=C—NH...HOOC— complexing during electrospinning. The formation of complexed structures with predominantly pyrrolidone amide group was also confirmed by shift of C=O carbonyl absorption band in NH-C=O (amide I band) from 1645 cm^{-1} for PVP/ODA-MMT nanofiber to 1652 cm^{-1} for all NFCs (Figures 2B, C and D). Absorption band at 1418 cm^{-1} was related to C-N stretching (amide III). The absorption bands at 2952 cm^{-1} and 2923 cm^{-1} were associated with C H stretching in CH2 groups from PVP and dextran units. Octadecyl group of organoclay and chain CH and CH_2 groups were confirmed with the presence of characteristic C H and CH_2 bending bands at 1462 cm^{-1} and 1423 cm^{-1}. The asymmetric Si-O-Si vibration with very strong and broad absorption band appeared in the 1104 cm^{-1} and 1008 cm^{-1}. Absorption band in 916 cm^{-1} could be attributed to Si O stretching from Si-OH (silica crystals at edges).

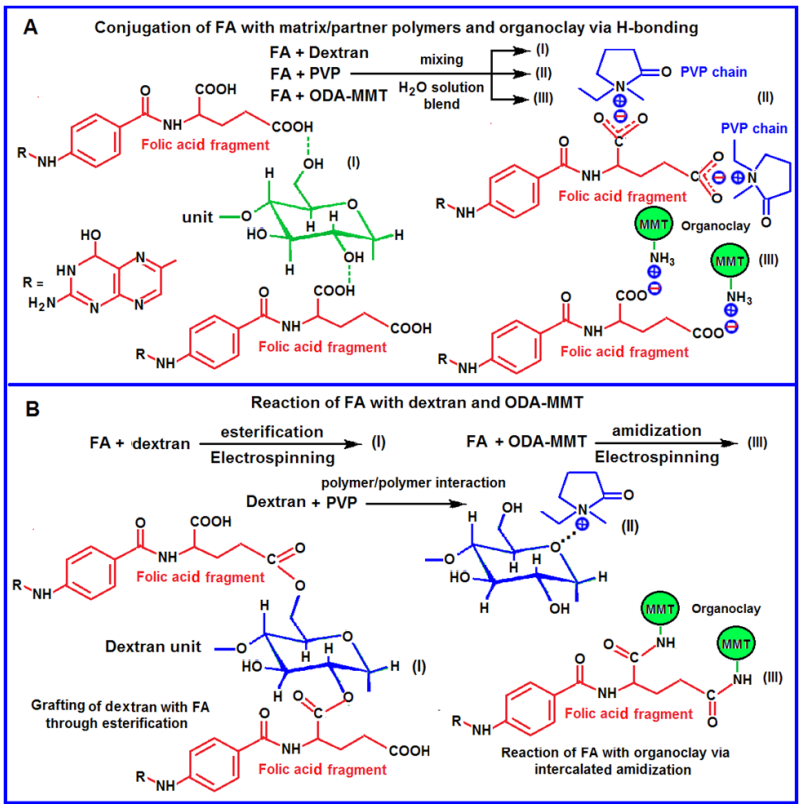

Figure 1. Schematic representation of (A) complexing physical reactions and (B) functionalization of dexran and organoclay via grafting with FA.

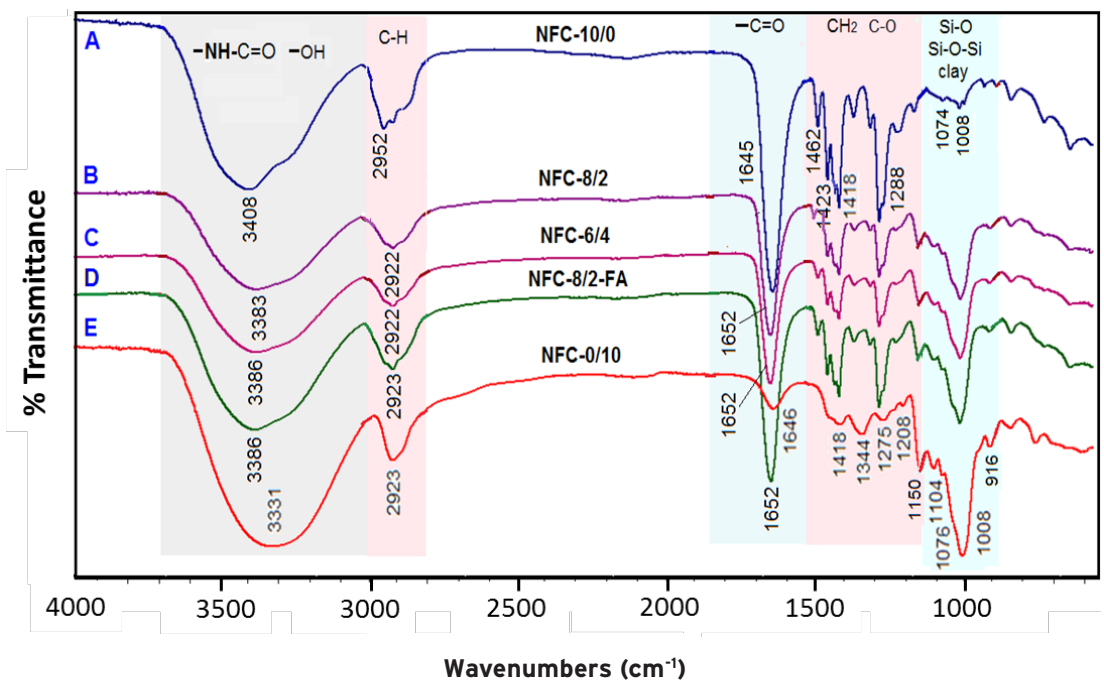

Figure 2. FT-IR spectra of NFCs from different volume ratios of NC-1/NC-2.

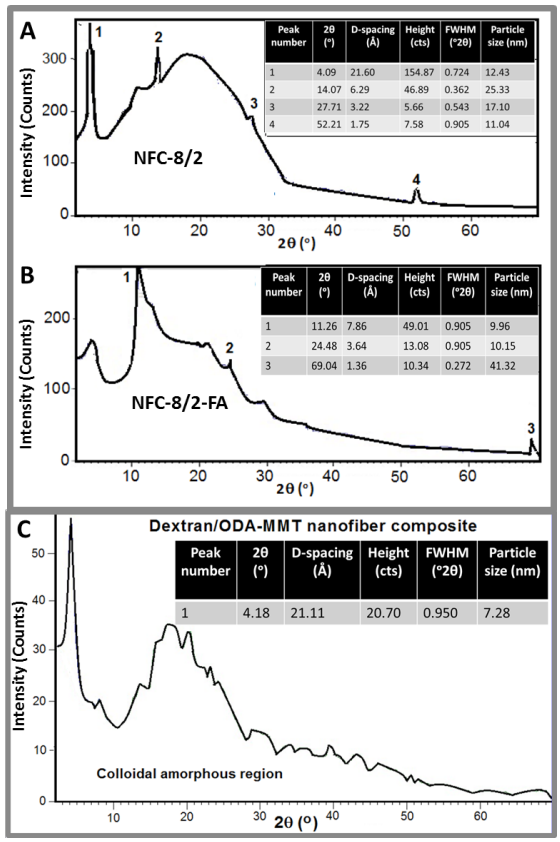

Figure 3. XRD patterns and X-ray reflection parameters of (A) NFC-8/2, (B) NFC-8/2-FA, and Dextran/ODA-MMT nanofiber composite.

Physical structures of NFCs were confirmed by XRD and are given in Figure 3. NFC-8/2 and NFC-8/2-FA predominantly exhibited amorphous structures with visible weak crystalline peaks at clay region which indicated the transfer of nanofiber structures to almost full colloidal state after partially elimination water molecules during electrospinning. Colloidal amorphous areas and visible crystalinite of NFCs were due to high swelling capacity of organoclay in water and complexing behaviors of organoclay and macromolecules of PVP and dextran in water medium, respectively. The reflection parameters were significantly changed in polymer and clay pattern regions around 2-30° 2θ angles. (Figures 3A and B). Disappearances of crystalline peaks in clay region (Figure 3C) and dramatically decrease in intensity polymer patterns with shifting to lower regions were detected. The reflection parameters of NFCs showed that an increase of partner polymer fraction in nanofiber film and conjugation of FA with fiber structures strongly improved colloidal amorphous areas and crystallinity (particle sizes). XRD results of dextran/ODA-MMT nanofiber composite showed that the nanofiber composite exhibited predominantly colloidal amorphous structure (Figure 3 C). The formation of a strong peak at 4.18° 2θ angle in the clay region with particle size 7.28 nm was related to silicate layers.

Surface Morphology of NFCs

SEM images of NFC films given in Figure 4 showed smooth and fine cross-section fiber morphology. However, an increase in dextran ratio in fibers resulted in the formation of some beaded fibers not affecting general morphology (Figure 4B). NFC-8/2, NFC-6/4, and NFC-8/2-FA had diameters of 379±240, 313±132, and 304±132, respectively. The addition of FA in polymer solution had an effect on reducing fiber diameter due to higher complexing behavior and chemical reactivity of FA molecules (Figure 4C).

In-vitro Cell Culture Studies

Cytotoxicity of the fiber samples (NFC-8/2 and

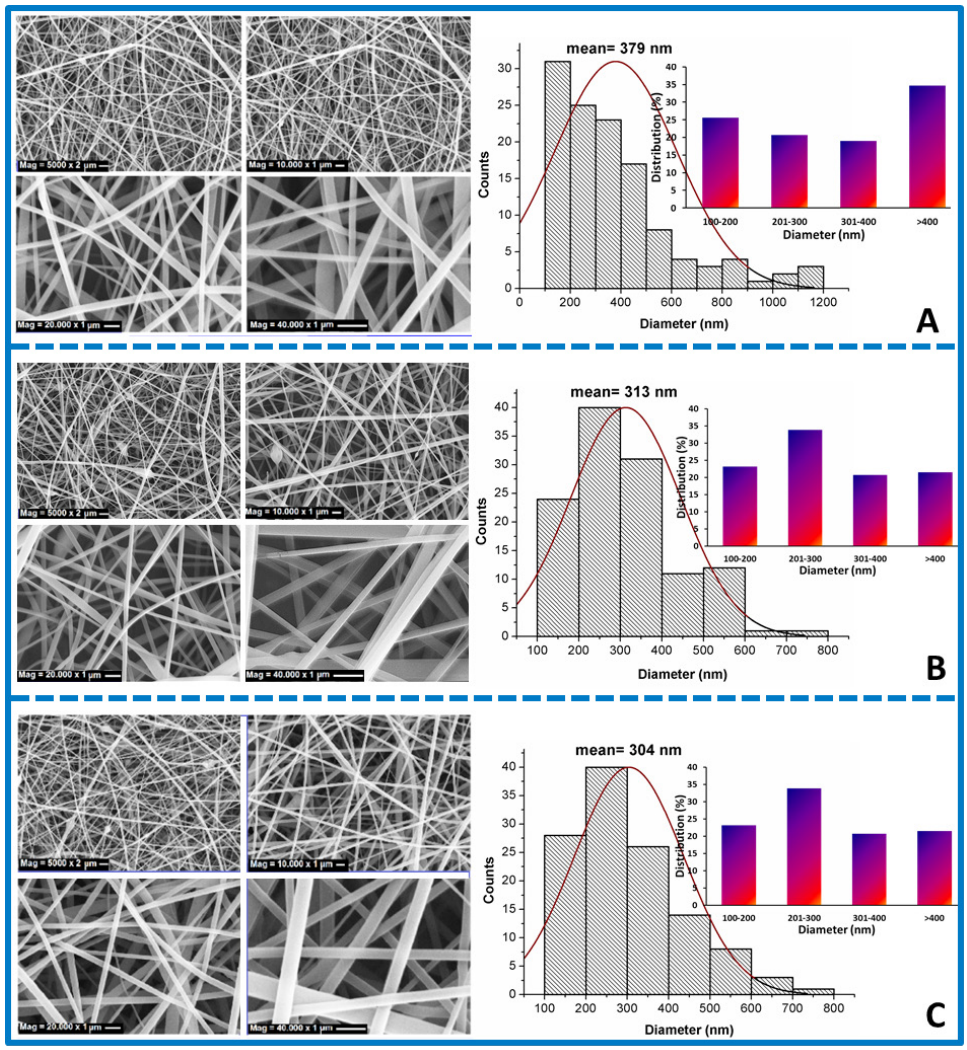

Figure 4. SEM images and diameter distributions of (A) NFC-8/2, (B) NFC-6/4, and (C) NFC-8/2-FA.

NFC-8/2-FA) at different concentrations to Vero cells are presented in the Figure 5. According to obtained results, no cytotoxic effect was observed on the samples in range of 12.5-200 µg/well, while the fibers exhibited low toxicity at the highest concentration for 48-hour of incubation. Cytotoxic evaluation of the cells on the samples showed that cell viability was in the range of 90-130% comparing with the control group.

The results of apoptotic and necrotic effects in the absence (control) and presence of NFCs are given in Figure 6. Apoptotic ratio obtained from average of the two methods was in the range from 2 to 6±1.5%. Thus, the result of double staining exhibited similar tendency to that of WST-1 test. According to the results, apoptotic effectiveness of NFC-8/2 and NFC-8/2-FA was low at all concentration levels and close-ranged with control group results. An increase in fiber amount did not cause an increase in apoptotic ratio. Figure 6 shows healthy, apoptotic, and necrotic cells under a fluorescent inverted microscope. Both healthy and apoptotic cell nucleuses are seen as blue color. However, apoptotic cell nuclei were stained with a stronger blue fluorescence compared to non-apoptotic cells (Figure 6B and E). Neither morphological changes nor apoptotic cells were seen in the control group (Figure 6A and C). When necrosis is examined with double straining method, Vero cells which are interacted with complexes from PI fluorescent dye are detected. This dye makes the cells viable under

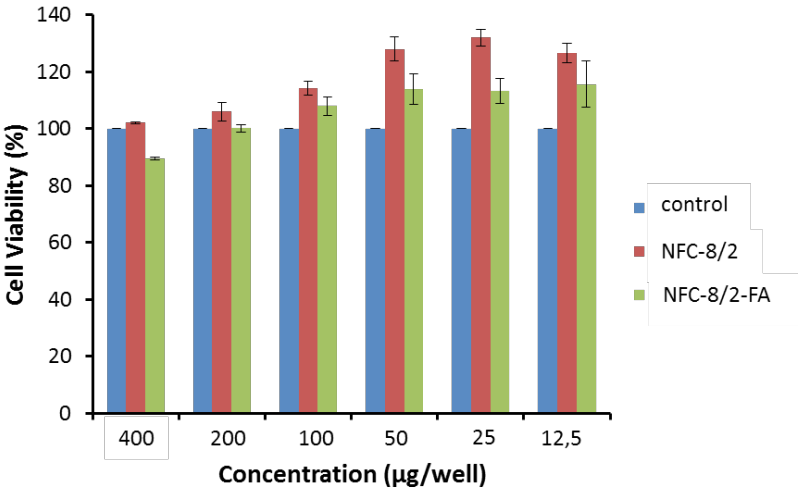

Figure 5. Cytotoxic effect of NFC-8/2 and NCF-8/2-FA on Vero cells *in vitro*.

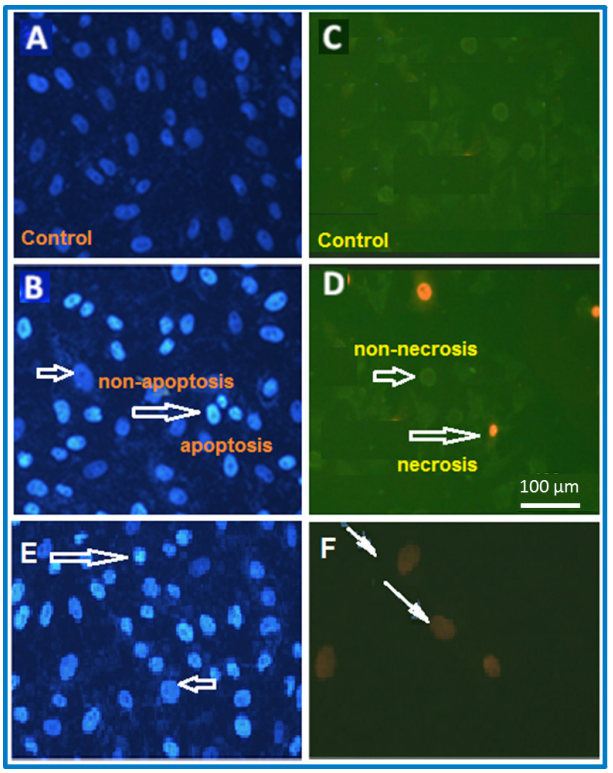

Figure 6. (A, B and E) Apoptototic and (C, D and F) necrotic images of the cells on (A and C) control, NFC-8/2 (B and D) and (E and F) NFC-8/2-FA from double staining (200 x, scale 100 µm).

red fluorescent light by passing through the dead cells only. In this study, the detection of necrotic indexes was examined in fluorescent light at 480-520 nm wavelengths. Nucleuses of necrotic cells were seen in red color between these wavelengths. The necrotic effects of NFC-8/2 and NFC-8/2-FA to the cells were close to each other and control group (Figure 6D and F). Necrotic cells about 3-5% ratios were observed at all used NFCs concentrations. In conclusion, an increase in the fiber amount did not led to significant effect on the cells. It was proposed that high polarity of the colloidal macromolecular complexes of PVP, dextran, organoclay and FA in culture medium provided no morphological changes Vero cells. Thus, excellent biocompatible NFCs exhibited low

toxicity and low degree of apoptotic and necrotic effects, and can be utilized for tissue engineering and other biomedical applications applications as platform/depositor.

CONCLUSIONS

This work presents the fabrication and characterization of novel biopolymer nanofiber composites from complexing water dispersed solution blends of biocompatible PVP/ODA-MMT, dextran biopolymer/ODA-MMT, and FA by green electrospinning nanotechnology. The dispersed blends of both biopolymer nanocomposites showed tendency to form hydrogen bonding with lower crystallinity and predominantly colloidal amorphous structures and good nanofiber properties. The results of cytotoxicity, apoptotic and necrotic analyses showed that the NFC films exhibit almost non-toxicity, low apoptosis and necrosis degree against Vero cell lines. It was suggested that NFCs fabricated and presented in this work at first time are promising candidates for cell culture, tissue engineering and various cancer cell lines applications which will be served as platform/depositors.

ACKNOWLEDGEMENT

The authors thank the Turkish Scientific and Technological Research Council (TUBITAK) for the financial support of this work through postdoctoral projects TBAG-HD/249 and BIDEB-PD/2218.

References

1. D.H. Reneker, I. Chun, Nanometer diameter fibres of polymer, produced by electrospinning, Nanotechnology, 7 (1996) 216-223.
2. W. E. Teo, S. Ramakrishna, A review on electrospinning. Design and nanofibre assemblies, Nanotechnology, 17 (2006) 89-106.
3. M. Şimşek, Z.M.O. Rzayev, S. Acar, B. Salamov, U. Bunyatova, Novel colloidal nanofiber electrolytes from PVA organoclay/poly (MA alt MVE), and their NaOH and Ag carrying polymer complexes, Polym. Eng. Sci. 56 (2015) 204-2013.
4. A. Arslan, M. Şimşek, S.D. Aldemir, N.M. Kazaroğlu, M. Gümüşderelioğlu, Honey-based PET or PET/chitosan fibrous wound dressings: effect of honey on electrospinning process, J Biomat. Sci.-Polym. E, 25 (2014) 999-1012.
5. R. Jayakumar, S.V. Nair, V. Beachley (eds.), Biomedical applications of polymeric nanofibers. In Book series: Advances in polymer science 246. Springer-Verlag: Heidelberg.
6. N. Saha, A. Saarai, N. Roy, T. Kitano, P. Saha, Polymeric biomaterial based hydrogels for biomedical applications, J. Biomater. Nanobiotechnol., 2 (2011) 85-90.
7. J. Xu, Y. Jiao, X. Shao, C. Zhou, Controlled dual release of hydrophobic and hydrophilic drugs from electrospun poly(l-lactic acid) fiber mats loaded with chitosan microspheres, Mater. Lett., 65 (2011) 2800–2803.
8. A.E. Deniz, H.A. Vural, B. Ortaç, T. Uyar, Gold nanoparticle/polymer nanofibrous composites by laser ablation and electrospinning, Mater. Lett., 65 (2011) 2941–2943.
9. W.E. Hennink, S.J. De Jongs, G.W. Bos, T.F.J. Veldhuis, C.F. Van Nostrum, Biodegradable dextran hydrogels crosslinked by stereocomplex formation for the controlled release of pharmaceutical proteins, Int. J. Pharm., 277 (2004) 99–104.
10. L. Hovgaard, H. Brondsted, Dextran hydrogels for colon-specific drug-delivery, J. Control Release, 36 (1995) 159–166.
11. S.G. Le´Vesque, M.S. Shoichet, Synthesis of cell-adhesive dextran hydrogels and macroporous scaffolds, Biomaterials, 27 (2006) 5277–5285.
12. S.G. Lévesque, R.M. Lim, M.S. Shoichet, Macroporous interconnected dextran scaffolds of controlled porosity for tissue-engineering applications, Biomaterials, 26 (2005), 7436–7446.
13. S.M. Naghib, M. Rabiee, E. Omidinia, P. Khoshkenar, D. Zeini (2012), Biofunctionalization of dextran-based polymeric film surface through enzyme immobilization for phenylalanine determination, Int. J. Electrochem. Sci. 7 (2012) 120-135.
14. Vasilis G. Gavalas, Nikolas A. Chaniotakis, Polyelectrolyte stabilized oxidase based biosensors: effect of diethylaminoethyl-dextran on the stabilization of glucose and lactate oxidases into porous conductive carbon, Anal. Chim. Acta, 404 (2000) 67–73.
15. J.F. Pan, N.H. Liu, H. Sun, Preparation and characterization of electrospun plcl/poloxamer nanofibers and dextran/gelatin hydrogels for skin tissue engineering, Plos One, 9 (2014) e112885.
16. R. Watadta, Y. Thaiying, Y. Saejeng, Y. Jaejeng, I. Jangchud, R. Rangkupan, C. Meechaisue, P. Supaphol, Electrospun dextran fibrous membranes, Cellulose, 15 (2008) 435-444.
17. H. Jiang, D. Fang, B.S. Hsiao, B. Chu, W. Chen, Optimization and characterization of dextran membranes prepared by electrospinning, Macromelecules, 5 (2004) 326-333.
18. M. Gadgil, K. Joshi, A. Pandit, S. Otiv, R. Joshi, J.T. Brenna, B Patwardhan, Imbalance of folic acid and vitamin B12 is associated with birth outcome: an Indian pregnant women study, Eur. J. Clin. Nutr., 68 (2014) 726-729.
19. B. Kamen, Folate and antifolate pharmacology. Seminar in oncology, 24, S18-S39, 1997.
20. R. Bargartz, Ag, M. Seleci, J.G. Walter, E. E. Yalcinkaya, O.D. Demirkol, F. Stahl, S. Timur, T. Scheper, Folic acid-modified clay: targeted surface design for cell culture applications, J. Mater. Chem. B, 1 (2013) 522-528.

21. F. Barlas, A. Ozkan, B. Demir, M. Seleci, M. Aydin, M. A. Taselen, H.Zareie, S. Timur, S. Ozcelik, Folic acid modified clay/polymer nanocomposites for selective cell adhesion, J. Mater. Chem. B, 2 (2014), 6412-6421.
22. Q.L. Jiang, S.W. Zheng, R.Y. Hang, S.M. Deng, L. Guo, R.L. Hu, B. Cao, M. Huang, L.F. Cheng, G.H. Liu, Y. Q. Wang, Folic ac*id*-conjugated Fe3O4 magnetic nanoparticles for hyperthermia and MRI *in vitro* an *in vivo*, Appl. Surf. Sci., 307 (2014) 224-233.
23. F.Ö. Gökmen, Zakir M.O. Rzayev, K. Salimi, U. Bunyatova, S. Acar, B. Salamov, M. Türk, Novel multifunctional colloidal carbohydrate nanofiber electrolytes with excellent conductivity and responses to bone cancer cells, Carbohydr. Polym., 133 (2015) 624–636.
24. K. Salimi, Z.M.O. Rzayev, E. Piskin, Functional Copolymer/Organo-MMT Nanoarchitectures. XXII. Interlamellar graft copolymerization of L-lactic acid onto poly(maleic anhydride-*alt*-1-octadecene) in the presence of different clays as catalyt-nanofillers. Journal of Appl. Clay Sci., 101 (2014) 106–118.
25. Zakir M.O. Rzayev, D. Erdönmez, K. Erkan, M. Şimşek, Ulviye Bunyatova. Functional Copolymer/Organo-MMT Nanoarchitectures. XXII. Fabrication and characterization of antifungal and antibacterial poly (vinyl alcohol-co-vinyl acetate/ODA-MMT/AgNPs nanofibers and nanocoatings by e-spinning and c-spinning methods, Int. J. Polymer. Mater., 64 (2015) 267-278.
26. Zakir M. Rzayev, Murat Şimşek, Koroush Salimi. Functional Copolymer/Organo-MMT Nanoarchitectures. XXVI. Fabrication and characterization of electrospun nanofibers from PCL/ODA-MMT and copolymer-g-PLA/Ag-MMT blends, Polym. Plast. Technol., 54 (2015) 1723-1734.